Nonadiabatic dynamics of electron injection into organic molecules*

Zhu Li-Ping(朱丽萍), Qiu Yu(邱 宇)†, and Tong Guo-Ping(童国平)

Department of Physics, Zhejiang Normal University, Jinhua 321004, *China*

(Received 18 December 2011; revised manuscript received 10 February 2012)

We numerically investigate the injection process of electrons from metal electrodes to one-dimensional organic molecules by combining the extended Su–Schrieffer–Heeger (SSH) model with a nonadiabatic dynamics method. It is found that a match between the Fermi level of electrodes and the highest occupied molecular orbital (HOMO) or the lowest unoccupied molecular orbital (LUMO) of organic molecules can be greatly affected by the length of the organic chains, which has a great impact on electron injection. The correlation between oligomers and electrodes is found to open more efficient channels for electron injection as compared with that in polymer/electrode structures. For oligomer/electrode structures, we show that the Schottky barrier essentially does not affect the electron injection as the electrode work function is smaller than a critical value. This means that the Schottky barrier is pinned for a small work-function electrode. For polymer/electrode structures, we find that it is possible for the Fermi level of electrodes to be pinned to the polaronic level. The condition under which the Fermi level of electrodes exceeds the polaronic level of polymers is shown to not always lead to spontaneous electron transfer from electrodes to polymers.

Keywords: nonadiabatic dynamics, electron injection, organic molecule

PACS: 73.40.–c, 71.38.–k **DOI:** 10.1088/1674-1056/21/7/077302

1. Introduction

In the past two decades, organic-based electronic devices, such as light-emitting diodes (LEDs)[1] and photovoltaic cells,[2,3] have attracted increasing interest because they have great processing and performance advantages when acting as displays and energy sources. Charge injection between metal electrodes and organic layers is thought to be one of the most significant issues that influence the device performance. There has been much research devoted to this field.[4−19] However, the charge injection is influenced by various factors and further studies on underlying mechanisms are still necessary.

Charge injection across the organic/electrode joints is dominated by the charge injection barrier, which involves the Schottky barrier and interfacial barrier arising from the interface dipole. Many experiments on the scheme of level alignment, which is believed to be determined by the combination of interfacial barrier and Schottky barrier, have been performed.[5−11] The Schottky barrier is determined by the relative difference between the Fermi level of electrodes and the LUMO (HOMO) of organic materials. Thus, the electronic structures of electrodes and organic layers dominate the Schottky barrier. In addition, charge transfer across the joint results in interface dipoles which have various origins such as a chemical reaction, contamination and direct electronic doping.[4] In all, the interfacial barrier can be markedly influenced by the process of sample preparation. The Schottky barrier has a complicated relationship with electrode work functions. For small molecules,[12] the Schottky barrier is pinned for low work-function electrodes, while it exhibits Schottky–Mott behavior for relatively high work-function electrodes. By contrast, for polymers[9] the Schottky barrier is linearly dependent on the electrode work function in the low regime. While in the high work-function regime, the Fermi levels of electrodes are pinned to the polaronic levels of polymers. As reported by Campbell *et al.*,[13] the metal electrodes do not introduce any interfacial states that pin the Schottky barrier in the single-particle gap. By contrast, it has been demonstrated by other experiments that the Fermi level is pinned to polaronic levels of a polymer, which is interpreted to occur as the electrode Fermi level is above (below) the negative (positive) polaron level.[9,10] For all the experimental endeavor, the measurement of level alignment is essentially accomplished

*Project supported by the National Natural Science Foundation of China (Grant Nos. 20974101 and 21174135).

†Corresponding author. E-mail: yqiu@zjnu.cn

© 2012 Chinese Physical Society and IOP Publishing Ltd

by the virtue of both the properties of materials and the interaction between them. Thus, it is not easy to find out how each of these factors affects the level alignment, respectively.

Organic/electrode structures have been extensively studied..[14−28] In the present work, we will show from a numerical point of view that metal electrodes can introduce localized states in the single-particle gap. However, conditions for the pinning of the Fermi level are not as simple as reported in Refs. [9] and [10]. To clarify these issues, we investigate the relaxation of electronic structures with the mean-field theory based on the SSH model[29] extended to organic/electrode coupling structures. The SSH model has been widely used to study organic molecule-based electronic transport and luminescence[30−35] and has provided quite a lot of insight into the carrier transport in intra-[36] and inter-molecules.[30] To understand the mechanism of the charge injection from metal electrodes into organic layers, it is very helpful to inspect the processes of spontaneous charge transfer.

In this paper, we numerically investigate the electron transfer from electrodes into organic molecules. The dynamics of charge transfer with respect to the electrode work function are investigated. The condition for the pinning of the Fermi level of polymer/electrode structures is clarified. The Schottky barrier is shown to be pinned for oligomer/electrode structures as the electrode work function is smaller than a critical value. The effect of an external electric field as well as the chain length on the charge injection is studied by using a nonadiabatic dynamic method.

2. Model and method

Organic molecules are described by the SSH model as one-dimensional (1D) chains,[29,37] where the interaction between electrons and lattices (e–l) plays an important role. The electrodes can also be described by the SSH model, but the electron–lattice coupling is neglected.[18,31] Typically, electronic devices contain some layers with different work functions. Chemisorption and/or surface contamination are brought into the joints in the preparation process. These factors can greatly affect the properties of the joints. In the present model, we take the organic/electrode joints as simple contacts and a coupling constant is introduced to reflect the correlation between the electrodes and the organic molecules. Thus, the SSH model can be extended as

$$H = H_{\rm e} + H_{\rm latt} + H_{\rm F}. \tag{1}$$

The electronic part is

$$H_{\rm e} = -\sum_{n,s} t_n (c^{\dagger}_{n,s} c_{n+1,s} + c^{\dagger}_{n+1,s} c_{n,s}) + \mu \sum_{n,s} c^{\dagger}_{n,s} c_{n,s}, \tag{2}$$

where $c_{n,s}$ ($c^{\dagger}_{n,s}$) denotes the electron annihilation (creation) operator at site n with spin s ($\uparrow$, $\downarrow$), and t_n is the hopping integral between sites n and $n+1$. For the electrodes, $t_n = t_0$, the organic molecules $t_n = t_0 - \alpha(u_{n+1} - u_n) + (-1)^{n+1} t_{\rm e}$, where u_n is the monomer displacement of site n, α is the coefficient of electron–lattice coupling, $t_{\rm e}$ is introduced to lift the ground-state degeneracy, and $t_n = t_{\rm c}$ reflects the coupling between sites connecting organic molecules and electrodes. μ is the chemical potential. For the organic molecules, the chemical potential is essentially zero throughout our numerical simulations. The lattice of the organic part is described as

$$H_{\rm latt} = \frac{K}{2} \sum_n (u_{n+1} - u_n)^2 + \frac{M}{2} \sum_n \dot{u}_n^2, \tag{3}$$

where K is the elastic constant and M the mass of the repeat monomer. The $H_{\rm F}$ describes the contribution from the external electric field and reads

$$H_{\rm F} = \sum_{n,s} V_n \left(c^{\dagger}_{n,s} c_{n,s} - \frac{1}{2} \right), \tag{4}$$

where V_n is the site energy due to the applied field, $V_n = |e|E[(n - n_0)a + u_n]$ with e being the electron charge, n_0 the first site of polymer chain, a the lattice constant, and E the uniform electric field.

For convenience, organic chains are assumed to be undoped. Thus, the chemical potential μ of the organic molecule part is zero provided that the virtual central level (VCL) of the gap is assigned as zero. If $\mu = 0$, the Fermi level and VCL of the electrodes align. It should be noted that the actual Fermi level of electrodes is a bit lower than the VCL because the number of monomers in the electrode is finite. Thus the eigen energy levels of the electrodes are discrete in the present model, as is schematically shown in Fig. 1. The electrode work function can be reduced by increasing the electrode chemical potential μ. The parameters in this model are those generally used in the SSH model for polyacetylene without loss of universality:[29,37] $\alpha = 4.1$ eV/Å, $K = 21$ eV/Å^2, $M = 1349.14$ eV·fs^2/Å^2, $t_0 = 2.5$ eV, $t_{\rm e} = 0.06$ eV, and $a = 1.22$Å. The interfacial coupling $t_{\rm c} = 1.0$ eV, indicating a relatively weak inter-chain charge transfer as compared with the intra-chain transfer t_0.

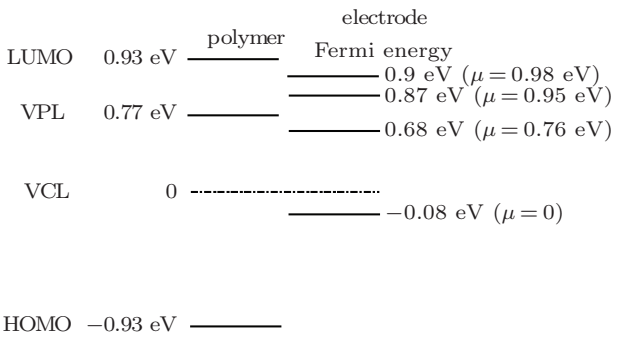


Fig. 1. Schematic diagram of electronic structure.

The charge transfer across the organic molecule/electrode contacts has been investigated using a dynamics method. The electronic wave functions evolve according to the Schrödinger equation

$$\begin{aligned} \mathrm{i}\hbar\dot{\psi}_i(n,t) = & -t_{n-1}\psi_i(n-1,t) + V_n\psi_i(n,t) \\ & - t_n\psi_i(n+1,t), \end{aligned} \tag{5}$$

where ψ_i can be expanded as a series of instantaneous eigenstates $\{|\varphi_\gamma\rangle\}$ which satisfy the following stationary Schrödinger equation:

$$H_\mathrm{e}|\varphi_\gamma\rangle = \varepsilon_\gamma|\varphi_\gamma\rangle, \tag{6}$$

$$|\psi_i(t)\rangle = \sum_\gamma |\varphi_\gamma\rangle\beta_{\gamma i}(t), \tag{7}$$

where $\beta_{\gamma i}$ are the expansion coefficients. The occupation number for the instantaneous eigenstate $|\varphi_\gamma\rangle$ is $n_\gamma = \sum\limits_i f_i|\beta_{\gamma i}|^2$, where f_i $(i = 0, 1, 2)$ is the time-independent distribution function determined by the initial electron occupation. The η for each eigenstate is defined as $\eta(\gamma) = \sum\limits_n |\varphi_\gamma(n)|^2$, where the index n runs over the sites of electrodes. As φ_γ is completely localized in the polymer, $\eta(\gamma)$ equals 0. On the other hand, if φ_γ is completely localized in the electrode, then $\eta(\gamma) = 1$. The value of $\eta(\gamma)$ is between 0 and 1, as φ_γ is a hybridized state. Based on the value of η, each electronic state can be clearly distinguished to be in the polymer or in the electrode. The lattice displacement of polymers is determined classically by using the Newtonian equation

$$\begin{aligned} M\ddot{u}_n = & -K(2u_n - u_{n+1} - u_{n-1}) \\ & + 2\alpha[\rho_{n,n+1}(t) - \rho_{n,n-1}(t)] \\ & + |e|E[\rho_{n,n}(t) - 1], \end{aligned} \tag{8}$$

where the density matrix ρ is defined as $\rho_{n,m}(t) = \sum\limits_i f_i\langle n|\psi_i(t)\rangle\langle\psi_i(t)|m\rangle$. The coupled differential equations (5) and (8) can be numerically solved by means of the same technique as that in Refs. [15], [30], [32], and [38]. In addition, $y_n \equiv (-1)^n(u_{n-1} + u_{n+1} - 2u_n)/4$ is defined to reflect the lattice configuration, and $\rho_n \equiv \rho_{n,n}$ denotes the charge distribution.

3. Results and discussion

3.1. Electron injection across polymer/electrode contacts

We consider a finite system containing 100 monomers in the polymer chain on the left side and 100 sites in the electrode attached on the right side. In the ground state, the polymer chain is dimerized due to the Peierls phase transition.[39] The energy gap for a 100-monomer chain is about 1.86 eV through a static iteration calculation,[32,40] and thus the value of LUMO is 0.93 eV. If an electron appears in the LUMO state, the electronic structure will change immediately due to the strong electron–lattice interaction. The LUMO will be lowered to form a binding state in the gap, i.e., a polaronic state.[41] The electronic energy of this state is about 0.77 eV. For the electrode, the actual Fermi level is calculated to be -0.08 eV when $\mu = 0$, as shown in Fig. 1. We start with a dimerized polymer chain contacted by an electrode with $\mu = 0.76$ eV. Once the coupling between the polymers and the electrodes is switched on, the electronic states are hybridized. Figure 2(a) shows the evolution of the total charge in both polymers and electrodes, from which we can see the polymer gains some charge of about 0.12 electrons and accordingly the electrode loses the same amount of charge. This result essentially indicates that the work function of the electrode is so large that there is little probability for the electrons to transfer into the polymer. A small amount of transferred charge is almost confined near the interface in the organic part, as shown in Fig. 2(b). If a forward bias ($E < 1.8 \times 10^6$ V/cm) is applied to the polymer, the total charge evolution diagram has no qualitative difference from those in Figs. 2(a) and 2(b). There is a very small increase in the amount of transferred charges. This indicates that small biases cannot switch on the charge injection. However, as the electric field is stronger than 1.8×10^6 V/cm, the situation changes. Figure 2(c) presents the total charge evolution in the case of $E = 2.5 \times 10^6$ V/cm. We can see that about 1.25 electrons are transferred from the electrode to the polymer. It is easier to be seen in Fig. 2(d) that the electron is injected into the polymer and quickly reaches the left side with the aid of the field, leading to a lattice deformation at the left-chain end, as indicated by the dashed line.

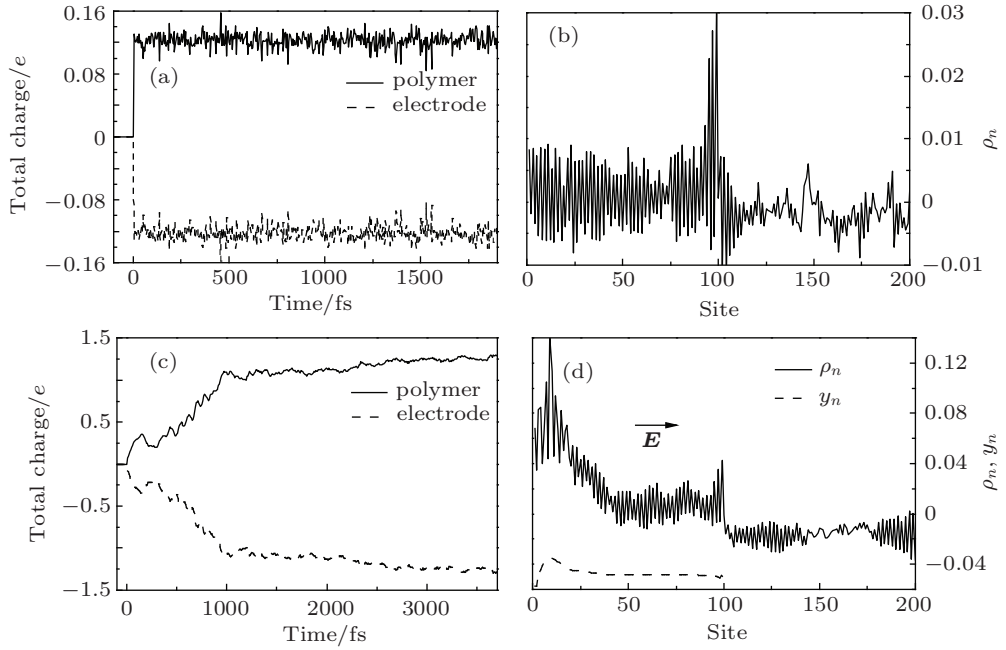


Fig. 2. Evolution of the total charge in the polymer and electrode (a) in the absence of an electric field and (c) in the presence of an electric field with $E = 2.5 \times 10^6$ V/cm. (b) Charge distribution ρ_n at $t = 500$ fs in the absence of an electric field. (d) Charge distribution ρ_n and lattice configuration y_n at $t = 100$ fs in the presence of an electric field with $E = 2.5 \times 10^6$ V/cm. The electrode $\mu = 0.76$ eV.

For $\mu = 0.76$ eV, the actual Fermi level of the electrode is 0.68 eV ((0.76–0.08) eV). The electrode work function is large enough so that the Fermi level of the electrode is lower than both the LUMO and the virtual polaron level (VPL). The VPL refers to the fact that if an electron is added to an organic molecule, there will be lattice deformation, forming a polaron in an organic molecule. In the energy space, the polaron level is below the LUMO which is shown in Fig. 1. As the electrode work function keeps reducing, the electrons are expected to be injected into the polymer with increasing probabilities. On this point, a numerical dynamics simulation is performed for $\mu = 0.98$ eV, as shown in Fig. 3. It should be noted that at $t < 0$ the coupling between the polymer and the electrode is turned off. Thus, they are both neutral as indicated in Fig. 3(a) by a total charge of zero for each. However, at $t = 0$, the coupling is turned on and the electrode μ increases from 0 to 0.98 eV. In Fig. 3(b), we can clearly see that an electron is injected into the polymer, forming a polaron quickly. In order to understand the microscopic picture of the charge injection process, we show the evolution of the 99th, 100th, and 101st eigen energy levels in Fig. 3(d). At $t < 0$, these three levels are all eigen levels of the electrode as shown in Fig. 3(e) with $\eta = 1$ for all the levels. The lower two levels are both occupied with two electrons with different spins. The 101st level is unoccupied, as shown in Fig. 3(f). However, if $t > 0$, the chemical potential of the electrode increases. As a result, as can be seen from Fig. 3(e), that after 200 fs the 99th state becomes an eigenstate mainly localized in the polymer. By contrast, the 100th and 101st states evolve into the eigenstates mainly localized in the electrode. From Fig. 3(f), it can be recognized that about 0.8 electrons occupy the 101st level and about 1.2 electrons occupy the 99th level, while about 2 electrons still occupy the 100th level. It should be noted that, during the evolution process, electrons are allowed to redistribute among the eigenstates of the polymer/electrode system. This process corresponds to the nonradiative decay process.[42,43] Thus, it is clear that the injected electrons mainly come from the enhanced Fermi surface, i.e., the 101st level. Within the first 200 fs, essentially the stage of electron injection, we can see that the occupation number as well as η undergo a drastic change. Originally, these changes come from the variation of instantaneous eigenstates, and thus of the Hamiltonian, the implicitly time-dependent factors of which are a set of monomer displacements. According to Eq. (8), the monomer displacement changes partially due to the electronic density matrix. Accordingly, the relaxation process is microscopically triggered by the electron–lattice interaction. The estab-

lishment of a correlation between polymers and electrodes eliminates the eigenstates that are completely localized in polymers or electrodes. All the electronic states turn to be hybridized states. Thus, the occupied states previously belonging to the electrode are likely to distribute on the polymer. This electronic distribution can effectively induce lattice deformation in the polymer. On the contrary, the deformed polymer lattice exhibits an attractive effect on the electron and the Schottky barrier is thus effectively reduced. In Fig. 3(c), it is shown that under a weak forward field ($E = 0.5 \times 10^5$ V/cm), the polaron moves away from the interface.

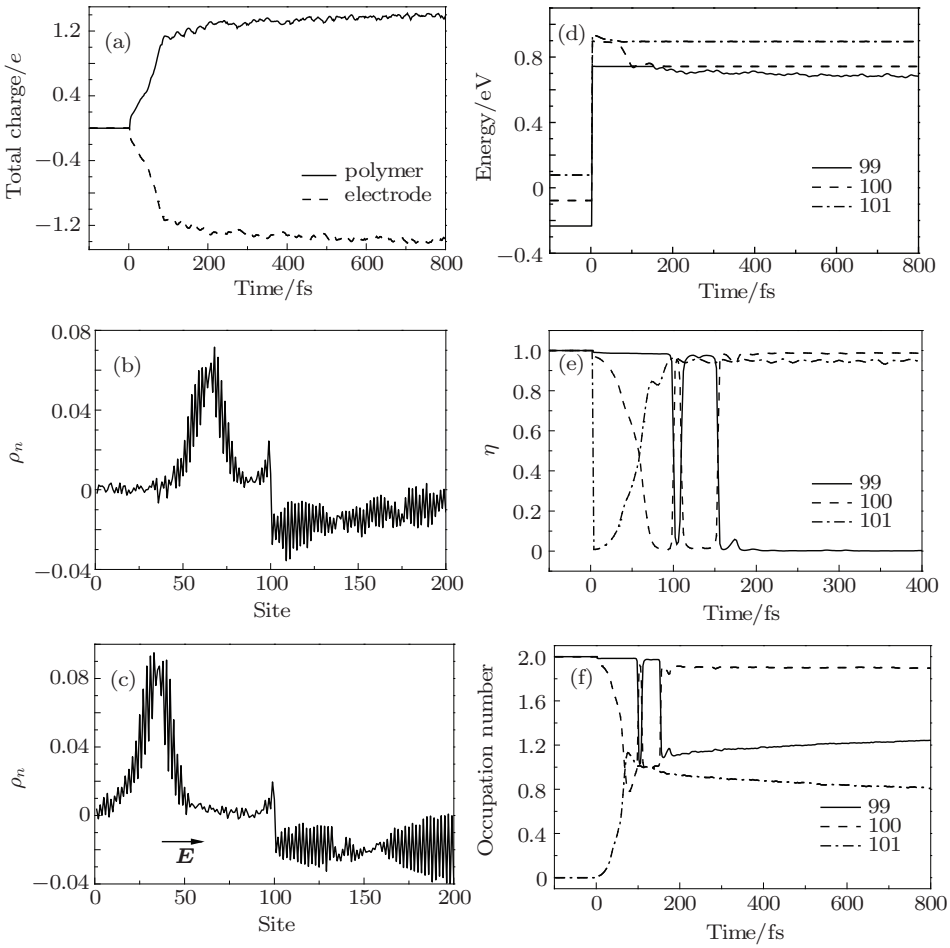


Fig. 3. Evolutions of (a) the total charge and (b) the charge distribution ρ_n at $t = 200$ fs in the absence of electric fields. (c) Charge distribution at $t = 230$ fs in the presence of the electric field with $E = 0.5 \times 10^5$ V/cm. Evolutions of (d) energy, (e) η, and (f) the occupation number of the 99th, 100th, and 101st eigen levels in the absence of electric fields. Electrode $\mu = 0.98$ eV.

To clarify the essence behind the fact that the Fermi level is pinned to the polaronic level,[9,10] we further perform simulations for $\mu = 0.95$ eV and the result is shown in Fig. 4. In this case, the electrode Fermi level is 0.87 eV, which is higher than the VPL but much lower than the LUMO as compared with that in the case of $\mu = 0.98$ eV. From Fig. 4, we can see that electrons cannot be injected into the polymer. Thus, the condition that the electrode Fermi level exceeds the polaron level of the polymer does not always lead to spontaneous electron transfer from electrodes to polymers. Therefore, we can conclude that the occurrence of charge injection in the case of $\mu = 0.98$ eV is not because the corresponding electrode Fermi level surpasses the VPL. It is the attractive impact upon electrons arising from the electron–lattice coupling in the polymer that effectively reduces the charge injection barrier and results in the spontaneous electron transfer.

It should be pointed out that although the parameters of the present model are those for polyacetylenes, our simulation results can be qualitatively applied to other conjugated polymers, such as poly (p-phenylene vinylene), because the energy-band structure of the latter can be readily obtained by adjusting the magnitude of parameters[44] provided that the effect of

molecular orientation is not taken into account.[45]

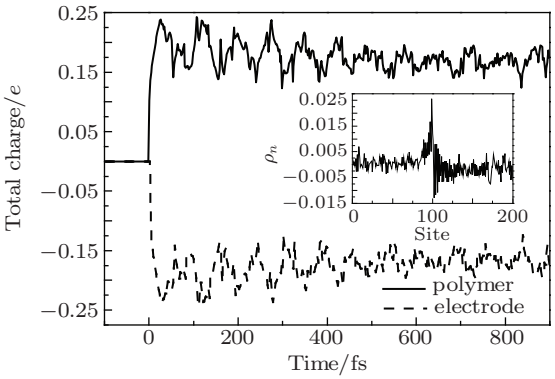


Fig. 4. Evolution of the total charge for electrode μ = 0.95 eV.

3.2. Electron injection across oligomer/electrode joints

In order to study the effect of chain length on electron injection, we consider an oligomer/electrode structure with 10 monomers in the oligomer and 100 sites in the electrode. Schematically shown in Fig. 5 is the electronic structure of the oligomer. The VBPL is the virtual bipolaronic level. Since in strong electron–lattice interaction systems, the attractive potential induced by electron–lattice coupling is much stronger than the Coulomb repulsive potential, the bipolaron level is lower than the polaron level.[37] Next we investigate the electron injection process for an electrode μ of 1.24 eV, given that the oligomer μ is still zero. Figure 6(a) describes the evolution of total charge in the oligomer and electrode. It is shown that at $t < 0$ the oligomer and electrode are both neutral because the coupling between them is turned off. At $t > 0$, the coupling is turned on and the electrode μ increases from 0 to 1.24 eV. About two electrons can be transferred from the electrode to the oligomer. To explore the origin of the charge transfer, we investigate the energy evolutions of the 52nd and 53rd eigen levels, as shown in Fig. 6(a). The evolutions of the occupation number and η of these two eigen levels are shown in Fig. 6(b). We can see from the curves of η that the two eigen states are both localized in the electrode at $t < 0$. When $t > 100$ fs, they show the same characteristics and distribute in both parts. About 35 percent of the 52nd eigen state distributes in the oligomer, while about 55 percent for the 53rd eigen state. Considering the occupation number of about 2 for both of the two eigen levels, these two states provide in total about 1.8 electrons in the oligomer. It can be seen from Fig. 6(a) that the average energy of these two levels is about 0.75 eV, which is very close to the VBPL. Therefore, the injected electrons actually lead to a bipolaron in the oligomer. It is noted that the electrode μ of 1.24 eV is the critical value, below which the charge injection does not occur. Compared with polymer, the critical electrode μ in the present oligomer case is very large. That is, the critical work function of the electrode that leads to efficient electron injection is very small in the oligomer case compared with the polymer case. As the electrode work function keeps reducing, our simulation results indicate that the electrons can be easily injected into the oligomer even if the electrode Fermi level is lower than the LUMO. The Schottky barrier becomes trivial in such cases and the interfacial barrier for electron injection in real cases is determined by some other factors irrelative to the electrode work function. In this sense, we can conclude that the Schottky barrier is pinned for small work-function electrodes.

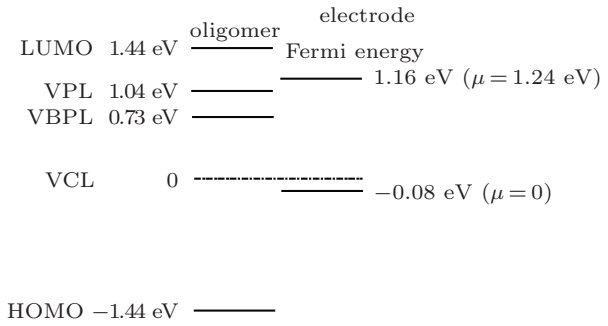


Fig. 5. Schematic diagram of electronic structure.

We have discussed that the electrode electrons are first injected into the LUMO and then they create localized deformations in the polymers. Since the electron–lattice coupling in polymers can effectively reduce the Schottky barrier, the electron injection can occur even if the electrode Fermi level is a bit lower than the LUMO. However, in the oligomer case, the critical Fermi level (1.16 eV as shown in Fig. 5) that leads to efficient electron injection is much lower than the LUMO, as compared with that in the polymer case. To clarify this issue, we investigate the effect of the correlation between oligomers and electrodes. Figure 7(a) shows the energy evolutions of the 64th and 65th eigen levels, and Fig. 7(b) shows the evolutions of η of these two levels, with $\mu = 0$ for both the oligomer and the electrode. $t = 0$ is still the off–on point of the correlation between the two parts. At $t < 0$, the 65th level is just the LUMO and the 64th level is the eigen level of the electrode which is occupied and lying in the gap nearest to the LUMO. At $t > 0$, the

eigen states of the oligomer/electrode system are all mixed states, which can be recognized by the variance of η of the 64th and 65th levels. The value of η for other eigen levels of the electrode lying in the gap at $t < 0$ almost remains unchanged (unit 1), which is not shown here. The decrease of η of the 64th eigen level actually opens an effective channel for the electron injection from electrodes into oligomers. Moreover, it is a more efficient channel for electron injection because the 64th level is much lower than the 65th one. That is, the electron-accepting levels in the oligomer is obviously lowered, which favors electron injection naturally. However, such effective injection channels are not found in polymer/electrode structures. In order to clarify the dependence of level alignment on the organic chain length, we perform simulations for organic molecules involving various monomers, keeping the electrode length invariant. For this purpose, we define ΔE as the energy difference between the LUMO of the organic molecule and the critical electrode μ. In Fig. 8, we show ΔE as a function of the organic chain length. It can be seen that with the decrease of the number of monomers in the organic molecule, ΔE increases nonlinearly. This indicates that the correlation between oligomers and electrodes opens more efficient channels for electron injection compared with that in polymer/electrode structures.

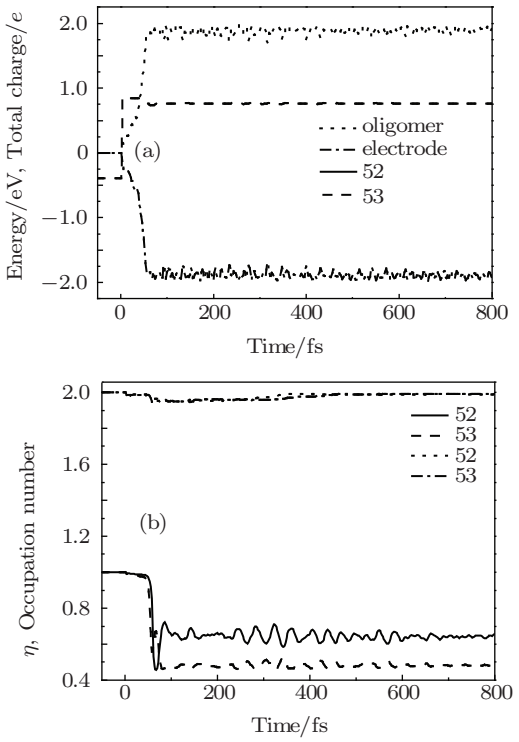


Fig. 6. (a) Energy evolution of the 52nd and 53rd eigen levels as well as evolution of the total charge in an oligomer and an electrode. (b) Evolution of η for the 52nd and 53rd eigen levels as well as evolution of the occupation number of the 52nd and 53rd eigen levels. Electrode $\mu = 1.24$ eV.

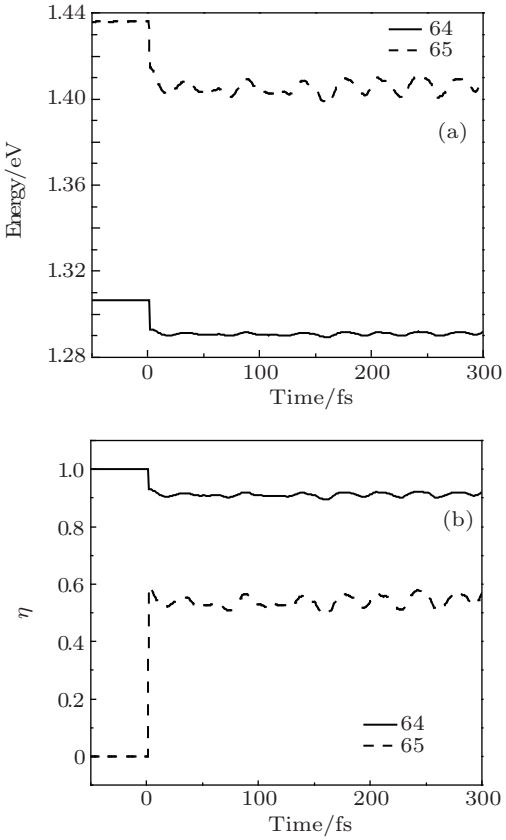


Fig. 7. (a) Energy evolution of the 64th and 65th eigen levels. (b) Evolution of η of the 64th and 65th eigen levels. Electrode $\mu = 0$.

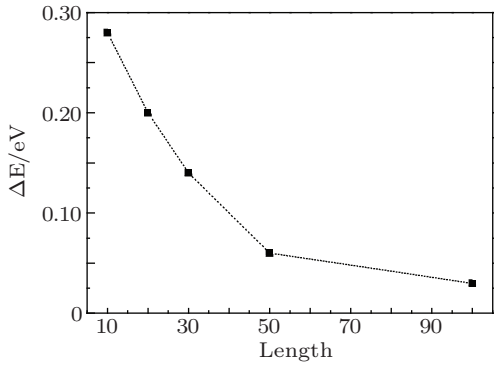


Fig. 8. ΔE with respect to the number of monomers in an organic molecule.

4. Conclusion

In summary, we have shown by numerical simulation that the match between the electrode Fermi level and the electron-accepting level of an organic molecule can be greatly affected by the organic chain length, which has an obvious effect on electron injection from electrodes to organic layers. The correlation

between oligomers and electrodes is shown to open more efficient channels for the electron injection compared with that in polymer/electrode structures. In addition, we have shown that an electric field stronger than a turn-on field favors the electron injection from electrodes into polymers, which is in agreement with experiments. The condition that the electrode Fermi level is higher than the polaron level of the polymer does not always lead to spontaneous electron transfer from electrodes to polymers. The coupling between electrodes and polymers results in hybridized states. The relaxation of these states gives rise to effective channels for electron injection even when the electrode Fermi level is lower than the LUMO of the polymer. For oligomer/electrode structures, the Schottky barrier is found to be pinned for small work-function electrodes.

It should be noted that the coupling strength of the electrodes and the organic layers obviously dominates the charge injection process in the present model. As the coupling strength is weak enough, charge injection will not take place. Our conclusions always hold as long as the charge injection channel is turned on. In addition, the electron injection is actually dominated by many aspects such as interfacial dipole and electron–electron interaction from a microscopic point of view. However, we put a particular emphasis on the effect of the organic chain length. Other effects are also important for the underlying mechanism and should be included in continued studies.

References

[1] Burroughes J H, Bradley D D C, Brown A R, Marks R N, Mackay K, Friend R H, Burn P L and Holmes A B 1990 *Nature* **347** 539

[2] Yu G, Gao J, Hummelen J C, Wudl F and Heeger A J 1995 *Science* **270** 1789

[3] Peumans P, Bulović V and Forrest S R 2000 *Appl. Phys. Lett.* **76** 2650

[4] Gao W and Kahn A 2003 *Appl. Phys. Lett.* **82** 4815

[5] Koch N, Kahn A, Ghijsen J, Pireaux J J, Schwartz J, Johnson R L and Elschner A 2003 *Appl. Phys. Lett.* **82** 70

[6] Narioka S, Ishii H, Yoshimura D, Sei M, Ouchi Y, Seki K, Hasegawa S, Miyazaki T, Harima Y and Yamashita K 1995 *Appl. Phys. Lett.* **67** 1899

[7] Hill I G, Rajagopal A, Kahn A and Hu Y 1998 *Appl. Phys. Lett.* **73** 662

[8] Veenstra S C, Stalmach U, Krasnikov V V, Hadziioannou G, Sonkman H T, Heeres A and Sawatzky G A 2000 *Appl. Phys. Lett.* **76** 2253

[9] Tengstedt C, Osikowicz W, Salaneck W R, Parker I D, Hsu C H and Fahlman M 2006 *Appl. Phys. Lett.* **88** 053502

[10] Crispin A, Crispin X, Fahlman M, Berggren M and Salanech W R 2006 *Appl. Phys. Lett.* **89** 213503

[11] Demirkan K, Mathew A, Weiland C, Yao Y, Rawlett A M, Tour J M and Opila R L 2008 *J. Chem. Phys.* **128** 074705

[12] Campbell I H and Smith D L 1999 *Appl. Phys. Lett.* **74** 561

[13] Campbell I H, Hagler T W, Smith D L and Ferraris J P 1996 *Phys. Rev. Lett.* **76** 1900

[14] Lei J, Li H, Jiang H and Xie S 2008 *Phys. Lett.* A **372** 6008

[15] Fu J, Ren J, Liu X, Liu D and Xie S 2006 *Phys. Rev.* B **73** 195401

[16] Davids P S, Saxena A and Smith D L 1996 *Phys. Rev.* B **53** 4823

[17] Samanta M P, Tian W, Datta S, Henderson J I and Kubiak C P 1996 *Phys. Rev.* B **53** R7626

[18] Yu Z G, Smith D L, Saxena A and Bishop A R 1999 *Phys. Rev.* B **59** 16001

[19] Basko D M and Conwell E M 2002 *Phys. Rev.* B **66** 094304

[20] Li D M, Yuan X J, Ma J S and Liu D S 2011 *Chin. Phys.* B **20** 117203

[21] Wang L F, Huang Q A, Tang J Y and Liao X P 2011 *Chin. Phys.* B **20** 037701

[22] Luo X Y, Zhang J H, Yan X J and Zhu G D 2010 *Chin. Phys.* B **19** 107702

[23] Hu Y and Rao H B 2009 *Chin. Phys.* B **18** 1627

[24] Li D M, Liu X J, Li Y, Li H D, Hu G C, Gao K, Liu D S and Xie S J 2008 *Chin. Phys.* B **17** 3067

[25] Feng W, Xu Y L, Yi W H, Zhou F, Wang X G and Yoshino K 2003 *Chin. Phys.* B **12** 426

[26] Li H H, Liu W and Liu D S 2011 *Acta Phys. Sin.* **60** 097201 (in Chinese)

[27] Nie G Z, Peng J B and Zhou R L 2011 *Acta Phys. Sin.* **60** 127304 (in Chinese)

[28] Li C, Peng J B and Zeng W J 2009 *Acta Phys. Sin.* **58** 1992 (in Chinese)

[29] Su W P, Schrieffer J R and Heeger A J 1979 *Phys. Rev. Lett.* **42** 1698

[30] Johansson A and Stafström S 2001 *Phys. Rev. Lett.* **86** 3602

[31] Wu C Q, Qiu Y, An Z and Nasu K 2003 *Phys. Rev.* B **68** 125416

[32] Li Y, Gao K, Sun Z, Yin S, Liu D S and Xie S J 2008 *Phys. Rev.* B **78** 014304

[33] An Z, Wu C Q and Sun X 2004 *Phys. Rev. Lett.* **93** 216407

[34] Sun X, Fu R L, Yonemitsu K and Nasu K 2000 *Phys. Rev. Lett.* **84** 2830

[35] Li S, George T F, He X, Xie B and Sun X 2009 *J. Phys. Chem.* B **113** 400

[36] Rakhmanova S V and Conwell E M 2000 *Synth. Met.* **110** 37

[37] Heeger A J, Kivelson S, Schrieffer J R and Su W P 1988 *Rev. Mod. Phys.* **60** 781

[38] Ono Y and Terai A 1990 *J. Phys. Soc. Jpn.* **59** 2893

[39] Peierls R E 1955 *Quantum Theory of Solids* (London: Oxford University Press)

[40] Stafström S 1985 *Phys. Rev.* B **31** 6058

[41] Mizes H A and Conwell E M 1995 *Synth. Met.* **68** 145

[42] Streitwolf H W 1998 *Phys. Rev.* B **58** 14356

[43] Johansson A A and Stafström S 2004 *Phys. Rev.* B **69** 235205

[44] Gao K, Liu X, Liu D and Xie S 2007 *Phys. Rev.* B **75** 205412

[45] Hultell M and Stafström S 2007 *Phys. Rev.* B **75** 104304